Feedback suppression of neural synchrony by vanishing stimulation

Natalia Tukhlina, Michael Rosenblum, Arkady Pikovsky, and Jürgen Kurths

Department of Physics, University of Potsdam, Am Neuen Palais 10, 14469, Potsdam, Germany[*]

(Received 25 July 2006; published 17 January 2007)

We suggest a method for suppression of collective synchrony in an ensemble of all-to-all interacting units. The suppression is achieved by organizing an interaction between the ensemble and a passive oscillator. Technically, this can be easily implemented by a simple feedback scheme. The important feature of our approach is that the feedback signal vanishes as soon as the control is successful. The technique is illustrated by the simulation of a model of an isolated population of neurons. We discuss the possible application of the technique in neuroscience.

I. INTRODUCTION

This work is motivated by the importance of macroscopic rhythmical neural activity in physiological and pathological brain functioning (see, e.g., Refs. [1–3], and references therein). In particular, well-pronounced brain rhythms, which are registered by means of electro-or magnetoencephalography in patients suffering from Parkinson's disease and essential tremor syndrome, cause the involuntary shaking of limbs, called tremor. Obviously, quenching of these rhythms constitutes an important clinical challenge. The technique, currently used in medical practice and known as *Deep Brain Stimulation (DBS)*, implies a *permanent* electrical stimulation of certain brain structures via implanted microelectrodes [4–6]. The mechanisms of DBS are yet poorly understood. To our knowledge, the only analysis of the action of high-frequency stimulation with the help of a realistic model of the brain circuitry involved in the tremor generation has been undertaken in Ref. [7].

A commonly used theoretical description of macroscopical brain rhythms assumes their appearance due to synchronization in a large population of interacting neurons [1]; this viewpoint is supported by experimental observations [8–11]. Because of a rich connectivity in such a population, the dynamics is often modeled by an ensemble of dynamical neurons with an all-to-all coupling. The simplest model for the synchronization in such an ensemble is a Kuramoto transition [12] in a population of all-to-all coupled phase oscillators. Correspondingly, the problem of suppression of neural synchrony is often formulated as the problem of *desynchronization of a large neuronal population* [1]. This means that the desired stimulation technique should not suppress oscillations of individual neurons, but only destroy the synchrony between them. Another important requirement is to minimize the intervention into the live system by reducing the intensity of the applied stimulation.

Several methods for a suppression of neural synchrony, closely related to the theoretical understanding of the problem, have been suggested recently. One theoretical approach to desynchronization is based on the implementation of phase resetting of ensemble elements by precisely timed pulses (see Refs. [1,13], and references therein), whereas another approach exploits a time-delayed feedback [14–17]. Although motivated by applications in neuroscience, both methods are of general interest, because a control of collective dynamics in a large population of units is not only relevant because of possible neuroscience applications, but represents an interesting physical problem. The mostly illustrative example of a physical system, where collective synchrony was highly undesirable and had to be suppressed, is the London Millennium bridge that exhibited high-amplitude lateral sway on the day of its opening [18,19]. We mention here also recent experiments on the desynchronization of a population of coupled electrochemical oscillators [20].

Our purpose in this paper is to develop and analyze an efficient technique for desynchronization in a population of interacting units. The main requirement for this method is to provide a *vanishing-stimulation control* [21]. That is, the magnitude of the control input (stimulation) $\mathcal{C}$ should be proportional to the synchronous rhythmic activity and must vanish as soon as the suppression is achieved. This can be accomplished by a feedback technique, where the control input decreases to the fluctuation level as soon as the rhythm is suppressed. Accordingly, we assume that in an experiment the mean field (or a related quantity, see Sec. III B) can be measured and subsequently used for stimulation of the ensemble via a feedback loop (see Fig. 1).

From a rather general physical viewpoint the population of neural oscillators to be controlled can be considered as an active medium. The main idea of our approach is to couple it to an *additional passive oscillator*. If we model the dynamics of the active medium by a single nonzero mode, then the problem is similar to a classical problem of the oscillation theory and nonlinear dynamics, where an interaction of an active, self-sustained oscillator, with a passive load (resonator) has been considered (see, e.g., Ref. [22]). It is known that under certain conditions such a passive system can quench the active oscillator. Similarly, the appearance of collective synchronization in a mixed population of active and passive oscillators depends on the proportion of passive elements; this effect, called aging, has been recently studied in Refs. [23,24]. However, in the context of neuroscience applications, a special consideration is necessary, because there appear three additional requirements to the suppression scheme: (i) the stimulation should compensate the unknown

_____

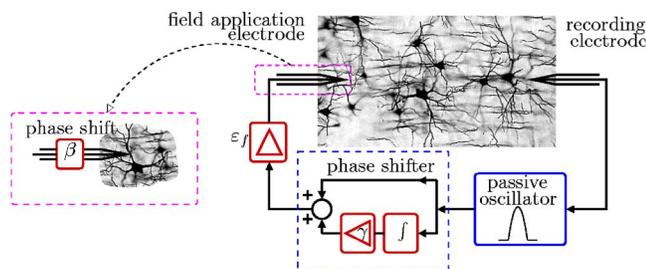*URL: www.agnld.uni-potsdam.de/~mros

FIG. 1. (Color online) Suggested suppression scheme. The local field potential related to the mean field of the population is measured by the recording electrode and is fed back via the field application electrode. The feedback loop contains a passive oscillator playing the role of a bandpass filter, an integrator, a summator, and two amplifiers. Stimulation is characterized by an *a priori* unknown phase shift.

phase shift inherent to stimulation (see Fig. 1 and the discussion below); (ii) the controller should be able to extract the relevant signal from its mixture with the rhythms produced by neighboring neuronal populations and with the measuremental noise; (iii) the control scheme should be able to compensate the *latency* in measurements. In our approach, presented below, we construct an auxiliary passive oscillator whose interaction with the ensemble of all-to-all coupled active units destroys the collective synchrony under the requirements formulated.

II. STABILIZATION OF AN ACTIVE OSCILLATOR BY A PASSIVE ONE

In this section we consider the stabilization problem on a macroscopic level, taking into account only the collective motion. In this way the problem is reduced to stabilization of a low-dimensional dynamics (see, e.g., Refs. [25–33], and references therein). However, the known techniques generally do not meet the above formulated requirements and therefore are not appropriate for the considered neuroscience application. Thus, we assume that the collective oscillating mode is active and close to a Hopf bifurcation,

$$\dot{A} = (\xi + i\omega)A - |A|^2 A + \mathcal{C}e^{i\beta}. \tag{1}$$

Here A is the complex amplitude of oscillations having frequency ω, ξ is the dimensionless parameter describing the instability of the equilibrium $A=0$, which we want to stabilize, and $\mathcal{C}$ is the control signal (stimulation). The parameter β describes the uncertainty of our action on the active oscillator: in a realistic application, the way the external force is coming in the equations is typically unknown.

Our aim is to construct the control signal $\mathcal{C}$ based on a scalar observable which, without lost of generality, can be chosen proportional to $X(t)=\text{const}+\text{Re}(A)$; here the constant reflects the fact that for neuronal models, the fixed point of collective oscillations is typically not at zero. (Note also that the case of other linear in A observable corresponds to a shift of the parameter β.) In Refs. [14,15] a time-delayed proportional feedback $\mathcal{C}\sim[X(t-\tau)-X(t)]$ has been suggested and treated numerically and analytically. Theory and simulation

with bursting and spiking neurons, also with synaptic connections [17], as well as recent experiment [20], show that such a control scheme provides a reliable suppression of oscillations, i.e., $\text{var}(X)\to 0$, with vanishing stimulation, $\mathcal{C} \to 0$. On the contrary, if a feedback is proportional to the delayed mean field, $\mathcal{C}\sim X(t-\tau)$ [14,15] or to its power [16,27,28], then the stimulation is generally not vanishing; i.e., a permanent stimulation with $\mathcal{C}=\text{const}$ is required for the maintenance of the suppressed state, $\text{var}(X)\to 0$. A general disadvantage of a delayed feedback is a new, undesirable, instability, which the delay term can bring into the system. To overcome this, we suggest a suppression scheme without delay, which exploits an additional passive oscillator.

The above-formulated requirements for the suppression can be now specified as follows: (i) a constant component in the observed field should be washed out; (ii) there should be a possibility to vary the phase shift in the feedback loop in a large range, to be able to compensate for the unknown phase factor β, and for a possible latency in the observations; (iii) noise and other components in the observed field, which are not related to the main rhythm should be washed out.

Let us include in the control loop a linear-damped oscillator in a way that it is driven by the measured signal,

$$\ddot{u} + \alpha\dot{u} + \omega_0^2 u = X(t). \tag{2}$$

The parameter ω_0 is taken to be equal to the frequency ω of macroscopic oscillations in Eq. (1) without control; this frequency can be easily measured in an experiment. This means that the driven oscillator (2) is in resonance with the forcing (for a moment we can consider it as a harmonic one with the frequency ω) and the phase of the output u is shifted by $\pi/2$ with respect to the phase of the input $X(t)$, whereas the phase shift of the derivative of the output signal $\dot{u}$ with respect to the input $X(t)$ is zero. It is important to note that the variable $\dot{u}$ does not contain a constant component, $\langle\dot{u}\rangle=0$, even if the observed field does. Thus, stimulation proportional to $\dot{u}$ vanishes as soon as the control is successful, and the requirement (i) to the control strategy is fulfilled. Moreover, the output $\dot{u}$ can be considered as an application of a bandpass filter to the input signal X, which filters out noise and other components outside of the vicinity of the main oscillation mode—this accomplishes the requirement (iii).

To compensate the unknown phase shift β [requirement (ii)] we include a unit described by the following equation:

$$\mu\dot{d} + d = \dot{u}. \tag{3}$$

For $\mu\omega\gg 1$ this unit operates as an integrator (with an additional multiplication by the factor $1/\mu$), whereas for $\mu\to 0$ its transfer function is 1. Hence, the output of system (3) has the same average as the input, i.e., $\langle d\rangle=0$. Finally, the control signal $\mathcal{C}$ is taken proportional to the weighted sum of $\dot{u}$ and d: $\mathcal{C}\varepsilon_f(\dot{u}+\gamma d)$, where the parameter γ determines the desired phase shift. The units performing this summation and the integration according to Eq. (3) form the *phase shifter*. It is seen from Fig. 2 that the phase difference θ between the output $\dot{u}+\gamma d$ of the phase shifter and its input $\dot{u}$ is
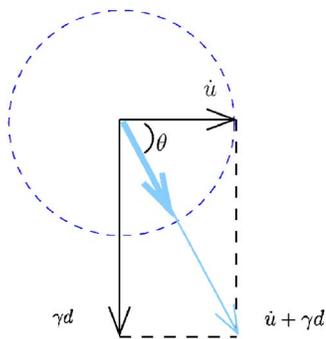
FIG. 2. (Color online) Illustration of the function of the phase shifter. The input to the shifter is represented by the vector $\dot{u}$. Integrator delays this input by $\pi/2$ and multiplies by $1/(\mu\omega)$; a result of this operation is represented by vector d. The output of the shifter is the sum $\dot{u}+\gamma d$. It is easy to see that the phase difference θ between the output of the phase shifter and its input is determined by the free parameter γ according to Eq. (4). For the stimulation we use the output (bold blue line), normalized by $\sqrt{1+\gamma^2/\omega^2\mu^2}$ [see Eq. (5)], which provides an independence of the amplification in the feedback loop from θ.

$$\theta = -\arctan\left(\frac{\gamma}{\omega\mu}\right), \tag{4}$$

and therefore can be arbitrarily varied in the interval $-\pi/2 < \theta < \pi/2$. The phase shift in the interval $\pi/2 < \theta < 3\pi/2$ can be obtained by the sign inversion: $\varepsilon_f \rightarrow -\varepsilon_f$. Summarizing, the control input $\mathcal{C}$ to the system is constructed as

$$\mathcal{C} = \pm\frac{\varepsilon_f}{\sqrt{1+\gamma^2/\omega^2\mu^2}}(\dot{u}+\gamma d) = \varepsilon_f\cos\theta(\dot{u}-\omega\mu d\tan\theta), \tag{5}$$

where $\sqrt{1+\gamma^2/\omega^2\mu^2}=1/\cos\theta$ is the normalization coefficient. It ensures an independence of the amplification in the feedback loop from the phase shift θ, so that this amplification is completely determined by ε_f. At the points $\theta=\pm\pi/2$ the control term is calculated as $\mathcal{C}=\varepsilon_f\omega\mu d$.

To complete the design of the control loop, we have to choose the parameter α, which is the damping factor of the oscillator (2). This parameter determines the width of the bandpass, $\Delta f=\alpha/2\pi$. Having in mind the application to Parkinsonian rhythms with realistic values for the bandpass from 10 to 13 Hz, we choose $\Delta f/f \approx 0.3$, which gives $\alpha =0.3\omega$.

The final equations for the controlled system read

$$\dot{A} = (\xi+i\omega)A - |A|^2 A + \frac{\varepsilon_f}{\sqrt{1+\gamma^2/\mu^2\omega^2}}(\dot{u}+\gamma d)e^{i\beta},$$

$$\ddot{u} + \alpha\dot{u} + \omega^2 u = \mathrm{Re}(A),$$

$$\mu\dot{d} + d = \dot{u}. \tag{6}$$

In the following we denote $\mathcal{E}=\varepsilon_f/\sqrt{1+\gamma^2/\mu^2\omega^2}=\varepsilon_f\cos\theta$.

The desired asynchronous state of the ensemble corresponds to the fixed point $A=0$ in the model equation. To analyze the stability of this solution, we consider only the
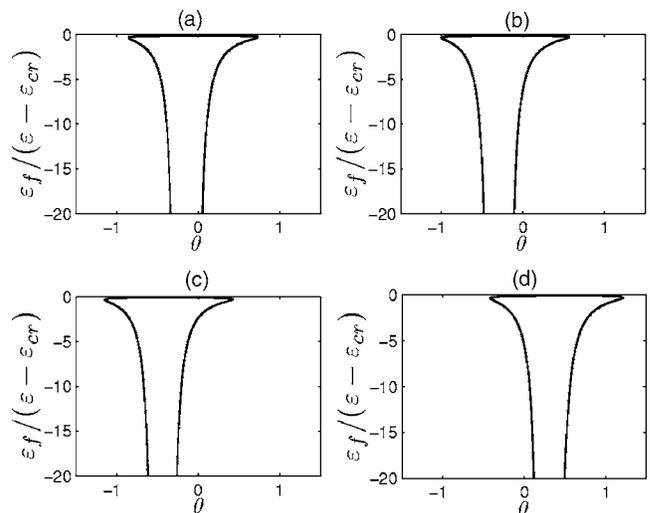

FIG. 3. Stability domains for the model equation (6) for different values of β. (a) $\beta=0$, (b) $\beta=\pi/20$, (c) $\beta=\pi/10$, (d) $\beta=-\pi/7$. The domains represent large, closed islands, which extend to large negative values of ε_f; only areas of strong stability are shown here.

linear terms of Eqs. (6), substitute $A=x+iy$ and $\dot{u}=v$, and rewrite the system Eqs. (6) as a system of five real differential equations of first order. Seeking the solution in the form $x=Xe^{\lambda t}$, $y=Ye^{\lambda t}$, $u=Ue^{\lambda t}$, $v=Ve^{\lambda t}$, $d=De^{\lambda t}$, we obtain the algebraic system of five linear equations. This system has a nontrivial solution if its determinant is equal to 0; this condition provides the equation $f(\lambda,\mathcal{E},\gamma)=0$ [its exact form is given by Eq. (A1)]. The border of the stability domain is determined by the condition $\mathrm{Re}(\lambda)=0$. Therefore, taking $\lambda =i\Omega$ on the stability border and separating real and imaginary parts, we obtain two real equations,

$$f_r(\Omega,\mathcal{E},\gamma) = 0,$$

$$f_i(\Omega,\mathcal{E},\gamma) = 0. \tag{7}$$

Both equations are linear with respect to $\mathcal{E}$ and γ. Therefore this system can be resolved with respect to γ and $\mathcal{E}$ and, with the account of Eq. (4) and $\varepsilon_f\cos\theta=\mathcal{E}$, rewritten as

$$\theta = \theta(\Omega),$$

$$\varepsilon_f = \varepsilon_f(\Omega). \tag{8}$$

These are the equations of the stability border in the parameter plane (θ,ε_f) in the parametric form; these lengthy expressions are given in the Appendix. Figure 3 shows stability domains according to Eqs. (8) for different values of the phase shift β and for the following values of the parameters: $\omega=2\pi/32.5$, $\alpha=0.3\omega$, $\mu=500$, $\xi=0.0048$. These parameters are chosen for comparison of the theory with the results of numerical simulation presented below. The domains quantitatively agree with the suppression domains, obtained in simulations of a stimulated ensemble of all-to-all coupled Bonhoeffer–van der Pol oscillators (see Figs. 5 and 6 below).

III. CONTROL OF SYNCHRONY IN NEURAL ENSEMBLES

To demonstrate the efficiency of our technique, we start by consideration of a simple model of collective synchrony. In a population of neurons each unit usually interacts with many other units, and, therefore, the collective dynamics is typically described by a mean-field model, which assumes a global (all-to-all) coupling between the elements. However, simulations with a Rulkov neuronal model [34] show that a randomly coupled population with a rather low connectivity of about 0.5% can be with a good precision described by a mean-field model [17].

A. Bonhoeffer–van der Pol oscillators

As the first example, we take an ensemble of N Bonhoeffer–van der Pol oscillators, coupled via the mean field in the x variable,

$$\dot{x}_i = x_i - x_i^3/3 - y_i + I_i + \varepsilon X,$$

$$\dot{y}_i = 0.1(x_i + 0.7 - 0.8y_i). \quad (9)$$

Here $i = 1, \ldots, N$ is the index of the neuron, $X = N^{-1}\Sigma_i x_i$ is the mean field, and the parameter ε quantifies the strength of the mean-field coupling. Let us first discuss the dynamics of the autonomous ensemble, i.e., the case when the stimulation is absent. The parameter I_i has the meaning of the external current and directly influences the spiking frequency of elements of the ensemble. They are not identical: the parameter I_i is taken as $I_i = 0.6 + \sigma$, where σ is a Gaussian-distributed number with zero mean and 0.1 rms value. For the coupling strength below the critical value, $\varepsilon < \varepsilon_{cr} \approx 0.018$, one observes small irregular fluctuations of the mean field X around $X_0 \approx -0.26$; these fluctuations are due to the finite size of the ensemble. With the increase of ε beyond the critical value $\varepsilon > \varepsilon_{cr} \approx 0.018$, the oscillators of the ensemble synchronize. Synchronization manifests itself via the appearance of a non-zero (macroscopic) oscillation of the mean field, whose amplitude grows with the supercriticality $\varepsilon - \varepsilon_{cr}$.

The stimulation $\mathcal{C}$ is modeled by including an additional term into the right-hand side of the Bonhoeffer–van der Pol model (9). However, in fact it is unknown, which variable, x or y, is affected by the stimulation. Therefore, for the generality, we assume that the stimulation is applied to both equations for x and y,

$$\dot{x}_i = x_i - x_i^3/3 - y_i + I_i + \varepsilon X + \mathcal{C} \cos \psi,$$

$$\dot{y}_i = 0.1(x_i + 0.7 - 0.8y_i) + \mathcal{C} \sin \psi, \quad (10)$$

where the parameter ψ governs the distribution of the stimulation between two equations. Note that the parameter ψ is related but not equal to the parameter β in Eq. (1). Indeed, as was shown in Ref. [15], even if $\psi = 0$, in the corresponding amplitude equation for the collective oscillations near the bifurcation point there appears a phase shift β, which is generally not zero. β is determined by the organization of global coupling in the ensemble and by the properties of individual units. This parameter characterizes the *a priori* unknown phase shift, inherent to the stimulation.
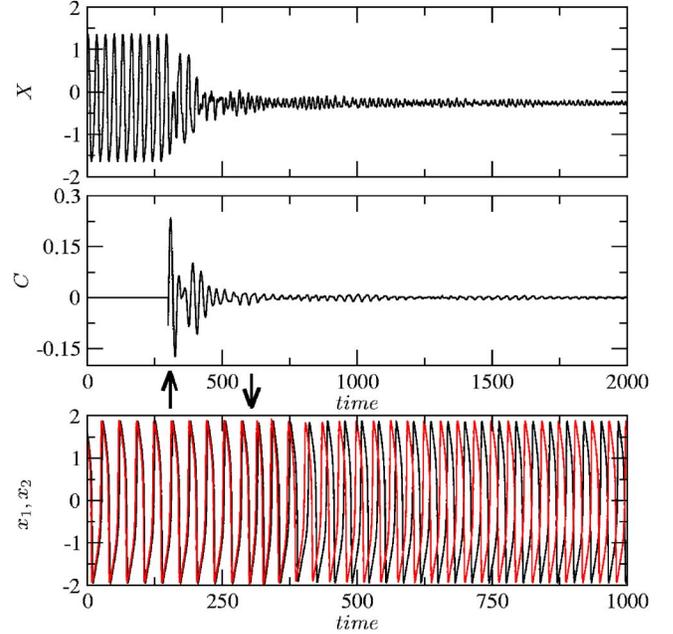

FIG. 4. (Color online) Suppression of synchrony in the population of Bonhoeffer–van der Pol oscillators, Eqs. (10). (a, b) The mean field X and the control signal $\mathcal{C}$ vs time. (c) Synchronous and asynchronous dynamics of two neurons in the absence and in the presence of the stimulation, respectively. The arrows indicate when the control is switched on.

We emphasize that model (10) is quite general, and, though we are speaking about interacting neurons here, our method can be applied to control the dynamics of a population of limit-cycle oscillators of any physical nature. On the other hand, model (10) lacks several important features specific for neuronal interaction. These features are considered in a more realistic model below.

We introduce the control loop via Eqs. (2), (3), and (5) above. We simulated the system (10) for $N = 10\,000$ and internal coupling $\varepsilon = 0.03$. The parameters of the bandpass filter are $\omega = 2\pi/32.5$, $\alpha = 0.3\omega$. The parameter of the integrator is $\mu = 500$. The results for $\beta = 0$, $\theta = 0$ are shown in Fig. 4. The control was switched on at $t_0 = 300$, i.e., $\varepsilon_f = 0$ for $t < t_0$ and $\varepsilon_f = -0.009$ for $t \geq t_0$. The panels (a) and (b) present the mean field and the control signal, respectively. It is seen that the stimulation results in a rapid suppression of the collective oscillation of the ensemble, where only small noiselike fluctuations remain. We quantify the suppression by the coefficient

$$S = \frac{\Delta X}{\Delta X_f},$$

where X and X_f are the mean fields in the absence and presence of the feedback, and ΔX and ΔX_f are their root mean square values, respectively. For the example shown in Fig. 4, we get $S = 157$. Generally, the suppression coefficient depends on the population size N like $S \sim \sqrt{N}$ (cf. Ref. [14]).

It is important that as soon as the suppression is achieved, the feedback signal practically vanishes, $\langle \mathcal{C} \rangle = -5 \times 10^{-6}$ and $\text{rms}(\mathcal{C}) = 0.0005$, to be compared to the amplitude of indi-
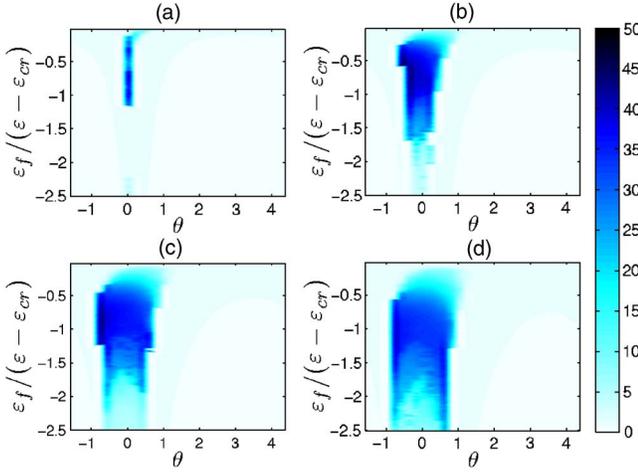
FIG. 5. (Color online) Domains of suppression for $N=500$ Bonhoeffer–van der Pol neurons (10) in dependence on the damping parameter α of the oscillator (2). The suppression factor S is shown in blue-scale coding. (a) $\alpha=0.1\omega$, (b) $\alpha=0.3\omega$, (c) $\alpha=0.5\omega$, (d) $\alpha=0.7\omega$. Note that only the regions with a relatively large suppression factor are shown: actually the stability domains extend for quite large negative values of ε_f (cf. Fig. 3).

FIG. 6. (Color online) Domains of suppression for $N=500$ Bonhoeffer–van der Pol neurons (10) for different values of the phase shift ψ: (a) $\psi=\pi/10$, (b) $\psi=\pi/20$, (c) $\psi=-\pi/7$, (d) $\psi=\pi/3$. These domains confirm that the phase shifter indeed ensures suppression. The damping parameter $\alpha=0.3\omega$. These numerical results agree with theoretical results (cf. Fig. 3).

vidual units ≈1.8. The dynamics of two neurons is shown in Fig. 4(c). One can see that the feedback control does not affect oscillations of individual units, but just destroys the synchrony between them so that they oscillate incoherently and therefore produce no macroscopic oscillation.

To illustrate the effect of damping parameter α of the filter on suppression we present in Fig. 5 the dependencies of the suppression coefficient S on θ, ε_f for an ensemble of $N=500$ Bonhoeffer–van der Pol oscillators (10); here $\psi=0$. The domains, where suppression is effective, represent closed, isolated areas. From these figures we can conclude that suppression of synchrony is observed for a relatively large parameter range. One can also see that with the increase of the damping parameter α, the suppression domains increase as well.

Figure 6 illustrates the functioning of the phase shifter. Here we show the suppression domains $S=S(\theta,\varepsilon_f)$ for different values of the phase shift ψ [see Eq. (10)]. For example, for $\psi=\pi/10$, the collective synchrony cannot be suppressed for $\theta=0$, i.e., the suppression is achieved only with the help of the phase shifter.

B. Desynchronization in a model of neuronal ensemble with synaptic coupling

In this section we make a step towards more realistic modeling of controlled neuronal dynamics. For the introductory example we used a quite abstract model (10); now we take into account several important features of the measurement of the collective neuronal activity and of the coupling between the neurons.

We have assumed that the collective activity of the population is reflected in the local field potential (LFP); the latter can be registered by an extracellular electrode. The question is how to relate the variab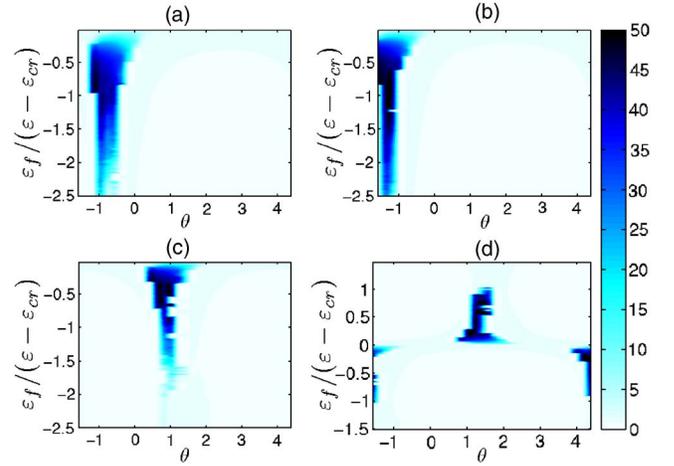les of conductance-based neuronal models to the LFP. The extracellular potential can be obtained via a solution of the Poisson equation with the membrane currents [35] determining the boundary condition [36,37]. Thus, the potential registered by the electrode is $\Phi \sim \Sigma_i(\mathcal{I}_i/r_i)$, where r_i is the distance between the current source, i.e., the membrane current of the ith neuron $\mathcal{I}_i$, and the measuring point. Hence, in the first approximation, neglecting the spatial structure of the ensemble, we can represent the measured signal as

$$\Phi \sim \sum_i \mathcal{I}_i. \qquad (11)$$

$\mathcal{I}_i$ is the right-hand side of the equation for the membrane potential V_i of a conductance-based neuronal model

$$C_i \frac{dV_i}{dt} = \mathcal{I}_i,$$

where C_i is the capacitance of the membrane. Note that $\mathcal{I}_i$ are the total membrane currents, which contain the currents through different ion channels and external currents, including the current due to stimulation. Using the notations of Eqs. (10), we can write $\Phi \sim \Sigma_i\mathcal{I}_i=\Sigma_i\dot{x}_i=N\dot{X}$. It means that the stimulation is now proportional to the derivative of the mean field.

Now we explore the efficacy of the suppression of collective rhythms in a neuronal ensemble with all-to-all synaptic connections. Indeed, interaction via the electrical (gap junction) coupling is possible only if the neurons are spatial neighbors [38]. Therefore, in a large network, where even spatially distant neurons can be synaptically linked by long axons, synaptic coupling plays a more important role.

Each neuron is modeled by the Hindmarsh-Rose equations [39], whereas the model and parameters of the inhibitory synaptic coupling are taken from Ref. [40]. Thus, the
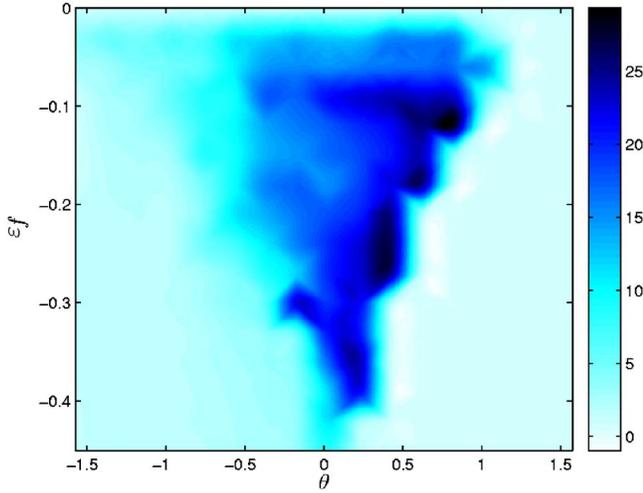
FIG. 7. (Color online) Domains of suppression for the ensemble of 200 synaptically coupled spiking Hindmarsh-Rose neurons [see Eq. (12)].

dynamics of the ensemble is described by the following set of equations:

$$\dot{x}_i = y_i + 3x_i^2 - x_i^3 - z_i + I_i - \frac{\varepsilon}{N-1}(x_i + V_c)$$

$$\times \sum_{j \neq i}^{N} \left[1 + \exp\left(\frac{x_j - x_0}{\eta} \right) \right]^{-1} + \mathcal{C},$$

$$\dot{y}_i = 1 - 5x_i^2 - y_i,$$

$$\dot{z}_i = r[\nu(x_i - \chi) - z_i], \tag{12}$$

where $r = 0.006$, $\nu = 1$, $\chi = -1.56$. ε is the strength of the synaptic coupling with the reverse potential $V_c = 1.4$; other parameters of synapses are $\eta = 0.01$, $x_0 = 0.85$. I_i is taken as $I_i = 4.2 + \sigma$, where σ is Gaussian distributed with zero mean and a 0.05 rms value. For zero coupling, each neuron exhibits regular spiking. With the increase of the synaptic coupling between the neurons, the model demonstrates a transition from independent firing to coherent collective activity [41]. In modeling the suppression, we again assume that the stimulation can be described as an additional external current, identical for all neurons. The LFP measurement is modeled according to Eq. (11). The result of simulation for $N = 200$ nonidentical inhibitory coupled neurons is presented in Fig. 7 for the following values of the parameters: $\varepsilon = 0.15$ and $\alpha = 0.3\omega$. The average frequency of the mean field is estimated as $\omega = 2\pi/3.82$. Note that in this model the mean action on each element *is not the mean field X*. Nevertheless, the measurement of $\dot{X}$ suffices to ensure desynchronization in the ensemble.

Finally, we consider the case when individual neurons exhibit chaotic bursting, i.e., generation of action potentials (spikes) alternates with the epochs of quiescence, so that the oscillation can be characterized by two time scales. This dynamics is provided by Eq. (12) with the following set of parameters: $r = 0.006$, $\nu = 4$, $\chi = -1.6$; the parameters of cou-
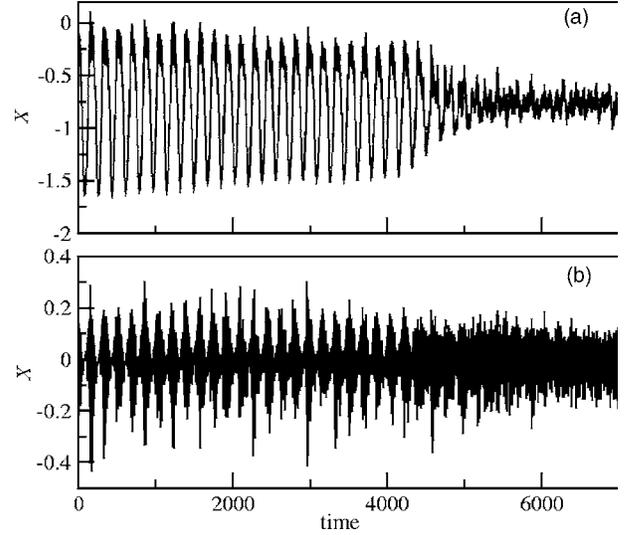

FIG. 8. (a) Mean field in an ensemble of synaptically coupled bursting Hindmarsh-Rose neurons is irregular but has a strong periodic component. The control has been switched on smoothly between $t = 3000$ and $t = 5000$. The suppression factor is $S = 6.5$, $\varepsilon_f = -0.12$, $\theta = -1.2$, $\alpha = 0.3\omega$. Note that for the measured signal we took the derivative of the mean field, shown in (b).

pling are kept the same as in the previous example. Synchronization occurs on the slower time scale, i.e., different neurons burst nearly at the same time, whereas the spiking within the bursts is not synchronous, and therefore is to a large extent averaged out in the mean field [Fig. 8(a)]. However, some high-frequency jitter remains due to correlations in spiking. As a result, the mean field is irregular; besides this jitter, it also exhibits a low-frequency modulation. The (average) frequency of the mean field is $\omega = 2\pi/176$; this corresponds to the interburst intervals.

Figure 8(a) demonstrates that though the mean field is irregular, it has a strong periodic component and therefore we expect that our technique is efficient in this case as well. This is indeed confirmed by the results of numerical simulation for $I_i = 3.2$, $\varepsilon = 0.2$, and various values of the damping parameter α (see Fig. 9 [42]). Again, the stability domains elongate for rather large negative values of ε_f and only parts of them, corresponding to stronger suppression, are shown. It can be seen that the increase of the damping parameter α, i.e., the increase of the bandwidth of the filter, leads to the extension of the suppression regions, similarly to the case of periodic oscillators (cf. Fig. 5). We conclude that suppression is possible in the case of irregular mean field as well, as long as the latter has a strong periodic component (what is expected if the system is not too far from the point of transition to synchronization). We are reminded that in order to simulate the measurement of LFP we use for stimulation the derivative of the mean field. This process [Fig. 8(b)] is even more complex than X; however, the suppression is achieved.

IV. CONCLUSIONS

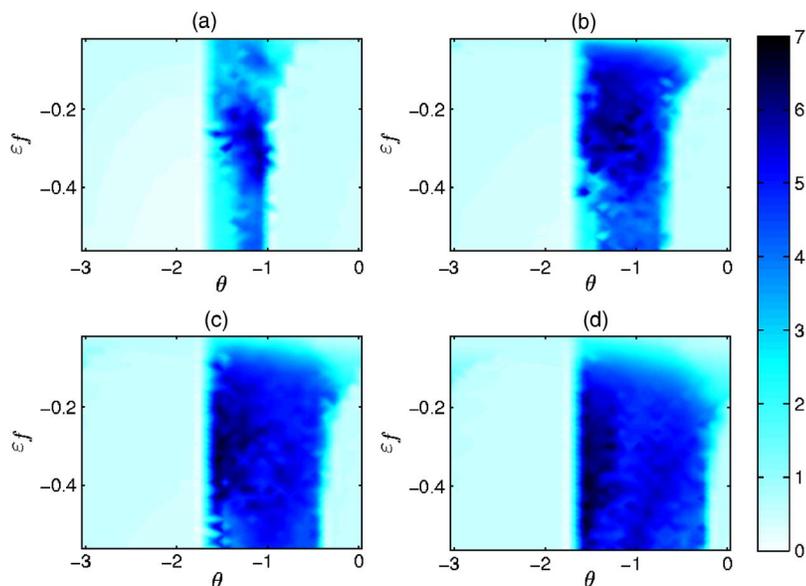We have proposed an efficient and simple technique for control of synchrony in a population of globally coupled

FIG. 9. (Color online) Domains of suppression for 200 bursting Hindmarsh-Rose neurons [Eq. (12)] for different values of the damping parameter α: (a) $\alpha=0.1\omega$, (b) $\alpha=0.3\omega$, (c) $\alpha=0.5\omega$, (d) $\alpha=0.7\omega$.

elements. Though we have concentrated on the problem of desynchronization, the technique can be also used for excitation of collective oscillation, if the coupling in the ensemble is subcritical and, thus, the uncontrolled system is stable. The suppression or excitation can be achieved if the total phase shift provided by the feedback loop is π or zero, respectively.

We hope that our technique can be used for the manipulation of neuronal rhythms, at least in an isolated population of neurons. This is confirmed by numerical simulations of a model of neuronal population. Important advantages of the technique are the simplicity of its practical implementation, built-in bandpass filter, and the ability to compensate the phase shift inherent to stimulation of the ensemble. We emphasize, that with our method we are able to stabilize the unknown steady state of the ensemble, which can also drift with time, and to maintain it by vanishingly small stimulation (cf. Refs. [28–30]). No knowledge of the properties of individual units and coupling between them is required. Finally, we remark that the latency in the measurement can be easily compensated by the phase shifter.

The suggested technique may possibly substitute delayed-feedback schemes in some other applications, e.g., in stabilization of low-dimensional systems [25–33], control of noise-induced oscillations [43], etc. As a problem for ongoing research we mention a development of an adaptive, self-tuning suppression technique.

APPENDIX: STABILITY DOMAIN OF THE MODEL EQUATION

The computation of the determinant of system (6) provides

$$
\begin{aligned}
&\lambda^5\mu + \lambda^4(1+\alpha\mu-2\xi\mu) + \lambda^3(\xi^2\mu-\mathcal{E}\mu\cos\beta+2\omega^2\mu \\
&\quad -2\xi\alpha\mu+\alpha-2\xi) + \lambda^2(\omega^2\alpha\mu-\mathcal{E}\cos\beta-\mathcal{E}\gamma\cos\beta \\
&\quad -2\xi\omega^2\mu-2\xi\alpha+\xi\mathcal{E}\mu\cos\beta+\xi^2\alpha\mu+\omega\mathcal{E}\mu\sin\beta+2\omega^2 \\
&\quad +\xi^2) + \lambda(\omega\mathcal{E}\sin\beta+\xi\mathcal{E}\cos\beta+\omega\mathcal{E}\gamma\sin\beta+\xi^2\omega^2\mu \\
&\quad +\omega^4\mu+\omega^2\alpha+\xi^2\alpha-2\xi\omega^2+\xi\mathcal{E}\gamma\cos\beta)+\xi^2\omega^2+\omega^4 \\
&= 0.
\end{aligned} \tag{A1}
$$

Stability domain in the parameter plane $(\gamma,\mathcal{E})$, or, equivalently in the parameter plane (θ,ε_f), is determined by the condition $\mathrm{Re}(\lambda)<0$. (We are reminded that $\gamma=-\omega\mu\tan\theta$ and $\mathcal{E}=\varepsilon_f\cos\theta$.) Taking $\lambda=i\Omega$ on the stability border and separating real and imaginary parts, we obtain

$$
\begin{aligned}
&\Omega^4(\alpha\mu+1-2\xi\mu) + \Omega^2[\mathcal{E}\cos\beta(1-\xi\mu+\gamma)-\omega\mu\mathcal{E}\sin\beta \\
&\quad +2\xi\alpha-2\omega^2-\xi^2+2\xi\omega^2\mu-\omega^2\alpha\mu-\xi^2\alpha\mu]+\omega^4+\xi^2\omega^2 \\
&= 0,
\end{aligned} \tag{A2}
$$

$$
\begin{aligned}
&\Omega\{\Omega^4\mu + \Omega^2[\mu(\mathcal{E}\cos\beta-\xi^2-2\omega^2+2\xi\alpha)+2\xi-\alpha]+\mathcal{E}(1 \\
&\quad +\gamma)(\omega\sin\beta+\xi\cos\beta)+\omega^2(\xi^2\mu+\alpha-2\xi)+\omega^4\mu \\
&\quad +\xi^2\alpha\} = 0.
\end{aligned} \tag{A3}
$$

Thus, we have two equations for two variables $(\gamma,\mathcal{E})$, and Ω is a parameter. It is easy to check that $\Omega=0$ provides no solution, therefore we divide Eq. (A3) by $\Omega\neq0$ and express $\mathcal{E}$ from this equation. Substituting it into Eq. (A2) we get γ. Then, substituting γ into the expression for $\mathcal{E}$ we finally obtain $\mathcal{E}$. Hence,

$$\gamma = A/B,$$

where

$$A = \omega \sin \beta [\Omega^6 \mu^2 + \Omega^4 (1 - 2\omega^2 \mu^2 + 2\mu^2 \xi\alpha - \mu^2 \xi^2)$$
$$+ \Omega^2 (\omega^2 \mu^2 \xi^2 - 2\omega^2 + \omega^4 \mu^2 + 2\xi\alpha - \xi^2) + \xi^2 \omega^2 + \omega^4]$$
$$+ \cos \beta [\Omega^6 (\alpha\mu^2 - \xi\mu^2) + \Omega^4 (\alpha - \xi - \xi^3 \mu^2 + \xi^2 \mu^2 \alpha$$
$$- \omega^2 \alpha\mu^2) + \Omega^2 (\xi^2 \alpha - \omega^2 \alpha - \xi^3 + \xi\mu^2 \omega^4 + \xi^3 \mu^2 \omega^2)$$
$$+ \xi^3 \omega^2 + \omega^4 \xi], \tag{A4}$$

$$B = \omega \sin \beta [\Omega^4 (2\xi\mu - \alpha\mu - 1) + \Omega^2 (\xi^2 \alpha\mu - 2\xi\omega^2 \mu - 2\xi\alpha$$
$$+ \xi^2 + \omega^2 + \omega^2 \alpha\mu) - \xi^2 \omega^2 - \omega^4] + \cos \beta [\Omega^6 \mu + \Omega^4 (\alpha\mu\xi$$
$$+ \xi^2 \mu - 2\omega^2 \mu + \xi - \alpha) + \Omega^2 (\omega^4 \mu - \xi^2 \omega^2 \mu + \omega^2 \alpha\mu\xi$$

$$+ \xi^3 \alpha\mu - \xi^2 \alpha + \omega^2 \alpha + \xi^3) - \xi^3 \omega^2 - \omega^4 \xi] \tag{A5}$$

and

$$\mathcal{E} = C/D,$$

where

$$C = \cos \beta [- \Omega^6 \mu + \Omega^4 (2\omega^2 \mu - \xi^2 \mu - \alpha\mu\xi + \alpha - \xi)$$
$$+ \Omega^2 (\xi^2 \omega^2 \mu - \xi^3 - \omega^4 \mu - \xi^3 \alpha\mu - \omega^2 \alpha\mu\xi + \xi^2 \alpha - \omega^2 \alpha)$$
$$+ \xi^3 \omega^2 + \omega^4 \xi] + \omega \sin \beta [\Omega^4 (1 - 2\xi\mu + \alpha\mu) + \Omega^2 (2\xi\alpha$$
$$+ 2\xi\omega^2 \mu - \omega^2 \alpha\mu - \xi^2 \alpha\mu - \xi^2 - 2\omega^2) + \omega^4 + \xi^2 \omega^2], \tag{A6}$$

$$D = \mu\Omega^2 [\xi\omega \sin 2\beta + \omega^2 + \cos^2 \beta (\Omega^2 + \xi^2 - \omega^2)]. \tag{A7}$$

---

[1] P. A. Tass, *Phase Resetting in Medicine and Biology. Stochastic Modelling and Data Analysis* (Springer-Verlag, Berlin, 1999).

[2] G. Buzsáki and A. Draguhn, Science **304**, 1926 (2004).

[3] *Epilepsy as a Dynamic Disease*, edited by J. Milton and P. Jung (Springer, Berlin, 2003).

[4] S. A. Chkhenkeli, Bull. Georgian Acad. Sci. **90**, 406 (1978).

[5] S. A. Chkhenkeli, in *Epilepsy as a Dynamic Disease*, edited by J. Milton and P. Jung (Springer, Berlin, 2003), pp. 249–261.

[6] A. Benabid *et al.*, Lancet **337**, 403 (1991).

[7] J. E. Rubin and D. Terman, J. Comput. Neurosci. **16**, 211 (2004).

[8] H. Bergman *et al.*, Trends Neurosci. **21**, 32 (1998).

[9] J. Sarnthein, A. Morel, A. von Stein, and D. Jeanmonod, Thalamus & Related Systems **2**, 321 (2003).

[10] J. A. Goldberg *et al.*, J. Neurosci. **24**, 6003 (2004).

[11] M. Magnin, A. Morel, and D. Jeanmonod, Neuroscience (Oxford) **96**, 549 (2000).

[12] Y. Kuramoto, *Chemical Oscillations, Waves and Turbulence* (Springer, Berlin, 1984).

[13] P. A. Tass, C. Hauptmann, and O. Popovych, Int. J. Bifurcation Chaos Appl. Sci. Eng. **16**, 7 (2006).

[14] M. G. Rosenblum and A. S. Pikovsky, Phys. Rev. Lett. **92**, 114102 (2004).

[15] M. Rosenblum and A. Pikovsky, Phys. Rev. E **70**, 041904 (2004).

[16] O. V. Popovych, C. Hauptmann, and P. A. Tass, Phys. Rev. Lett. **94**, 164102 (2005).

[17] M. Rosenblum, L. Cimponeriu, N. Tukhlina, and A. Pikovsky, Int. J. Bifurcation Chaos Appl. Sci. Eng. **16**, 7 (2006).

[18] S. H. Strogatz *et al.*, Nature (London) **438**, 43 (2005).

[19] P. Dallard *et al.*, J. Bridge Eng. **6**, 412 (2001).

[20] J. Hudson (private communication).

[21] In the context of chaos control the schemes with a vanishing feedback signal are sometimes called noninvasive. Having in mind possible applications in neuroscience, we prefer not to use this term here, because in this field any measurement (stimulation) using implanted electrodes is considered as invasive.

[22] P. S. Landa, *Self-Oscillations in Systems with Finite Number of Degrees of Freedom* (*Nauka*, Moscow, 1980), in Russian.

[23] H. Daido and K. Nakanishi, Phys. Rev. Lett. **93**, 104101 (2004).

[24] D. Pazó and E. Montbrió, Phys. Rev. E **73**, 055202(R) (2006).

[25] K. Pyragas, Phys. Lett. A **170**, 421 (1992).

[26] D. V. R. Reddy, A. Sen, and G. L. Johnston, Physica D **144**, 335 (2000).

[27] F. M. Atay, Int. J. Control **75**, 297 (2002).

[28] F. M. Atay, *Dynamics, Bifurcation, and Control*, Lecture Notes in Control and Information Sciences Vol. 273 (Springer-Verlag, Berlin, 2002), pp. 103–116.

[29] M. A. Hassouneh, H.-C. Lee, and E. H. Abed, *Proceedings of the 2004 American Control Conference* (AACC, Boston, MA, 2004), pp. 3950–3955.

[30] M. A. Hassouneh, H.-C. Lee, and E. H. Abed, Technical report, Institute for Systems Research (unpublished).

[31] K. Pyragas *et al.*, Phys. Rev. E **70**, 026215 (2004).

[32] P. Hövel and E. Schöll, Phys. Rev. E **72**, 046203 (2005).

[33] J. Bechhoefer, Rev. Mod. Phys. **77**, 783 (2005).

[34] N. F. Rulkov, Phys. Rev. Lett. **86**, 183 (2001).

[35] These currents are due to the motion of ions from the extracellular space into the cells and back.

[36] U. Mitzdorf, Physiol. Rev. **65**, 37 (1985).

[37] P. beim Graben, Ph.D. thesis, Universität Potsdam, 2000 (unpublished).

[38] The electrical coupling is a usual resistive coupling; it is possible only if the interacting neurons are closely spaced.

[39] J. L. Hindmarsh and R. M. Rose, Proc. R. Soc. London, Ser. B **221**, 87 (1984).

[40] R. Huerta, M. I. Rabinovich, H. D. I. Abarbanel, and M. Bazhenov, Phys. Rev. E **55**, R2108 (1997).

[41] The dynamics of the coherent activity is quite complicated, however, it can be suppressed.

[42] Note that in order to avoid a large current pulse at the beginning of the stimulation, the latter is switched on in a smooth way.

[43] N. B. Janson, A. G. Balanov, and E. Schöll, Phys. Rev. Lett. **93**, 010601 (2004).